AN ABSTRACT OF THE THESIS OF

PAUL MORRIS FLUGSTAD (Name of student) for the M. S. (Degree)

in Chemistry (Analytical) (Major) presented on July 29, 1968

Title: INVESTIGATION OF THE RELATIONSHIPS BETWEEN LASER ENERGY AND VAPORIZED TARGET MATERIAL, CONTINUUM INTENSITY, AND PLUME ENERGY IN LASER PLUME SPECTROSCOPY

Redacted for Privacy

Abstract approved: Edward H. Piepmeier

A focused Q-switched neodymium-doped glass laser with power levels ranging from 1-6 MW and with a 50-nsec halfwidth, was used to vaporize copper metal. Experimental measurements showed that the amount of material vaporized away from the target was not linear with laser power and was much less than could be accounted for by the laser energy available. Amounts of copper in the 0.0X μg range were measured for the power range investigated. Experimental methods are described to monitor the power and energy of the laser beam as the target material was vaporized and collected for measurement.

Photodiode monitors were built to measure simultaneously the plume plasma continuum intensity and the laser beam power and energy. The measurements showed a linear increase in the plume

continuum emission as a function of laser beam power. The total emission seen by the photodiode was shown to be approximately linearly related to the energy transferred to the plume plasma.

The energy that could not be accounted for by the vaporized material was shown, using reasonable assumptions, to be governed by the laser beam energy losses to the plume plasma. The shape of the theoretically calculated curve was found to be consistent with the experimental measurements, giving evidence that energy is being transferred to the plume plasma approximately linearly as a function of laser beam power. This energy might otherwise have been used in vaporizing target material for analytical purposes.

Investigation of the Relationships between Laser Energy and Vaporized Target Material, Continuum Intensity, and Plume Energy in Laser Plume Spectroscopy

by

Paul Morris Flugstad

A THESIS

submitted to

Oregon State University

in partial fulfillment of
the requirements for the
degree of

Master of Science

June 1969

APPROVED:

Redacted for Privacy

Assistant Professor of Chemistry
in charge of major

Redacted for Privacy

Head of Department of Chemistry

Redacted for Privacy

Dean of Graduate School

Date thesis is presented July 29, 1968

Typed by Opal Grossnicklaus for Paul Morris Flugstad

ACKNOWLEDGMENT

The author wishes to express his gratitude to Dr. Edward Piepmeier for his help, guidance and encouragement throughout the course of this work.

Appreciation is also extended to the National Aeronautics and Space Administration for their support in this work, through a fellowship awarded to the author.

Appreciation is also due to Dr. Donald Reed for his suggestions on the manuscript.

Finally, the author wishes to thank his parents, Edith and Morris Flugstad, for their many contributions to his education.

TABLE OF CONTENTS

LIST OF FIGURES

INVESTIGATION OF THE RELATIONSHIPS BETWEEN LASER ENERGY AND VAPORIZED TARGET MATERIAL, CONTINUUM INTENSITY, AND PLUME ENERGY IN LASER PLUME SPECTROSCOPY

I. INTRODUCTION

Because of the ability to focus a laser beam on a small area, scientists have been interested in using the laser as a source of energy for vaporization and excitation of a sample in highly localized spectrochemical analysis. The method has been used with samples ranging from metals and semiconductors to biological material, such as cells. Because of the lack of understanding of the sampling and excitation processes, much time is spent in empirically establishing analytical parameters for each new and different analysis.

In order to improve this method of analysis and make it easier to interpret the results, it is necessary to investigate the method of energy transfer from the laser beam to the target species, together with the amount of material sampled, background continuum emission, and energy losses to the plume plasma as a function of laser beam energy and power. This would not only help an investigator in his efforts to obtain optimum accuracy, sensitivity and reproducibility for a given analysis, but also would help him to predict what parameters might be best for future and different analyses.

Because, analytically it is important to know how the sampling

conditions vary with laser beam power and energy, measurements were made of the amount of material vaporized away from the target as a function of laser beam power and energy. Measurements were also made of the continuum background of the plume plasma at different laser powers and energies. From these measurements, the amount of energy lost to the plume plasma was estimated. The analytical significance of the results of these measurements is discussed.

II. HISTORICAL

In the last few years, there has been much interest in understanding the processes occurring when the laser beam hits the target material. Two types of laser pulses have been used. The normal laser pulse consists of tens to hundreds of randomly spaced laser spikes with different peak powers normally in the kilowatt range. The Q-switched or giant pulse laser consists of one to a few spikes of 10-100 nsec halfwidth in the kilowatt to megawatt power region. Work (13) has shown that the Q-switched spikes may consist of several 1-nsec laser spikes spaced a few nanoseconds apart.

Q-switched laser spikes have been found to be more reproducible and easier to synchronize on a submicrosecond scale with the rest of an experiment, than the normal laser pulses. As a result, most work to date has been done with this type of laser. Some work has also been done with the normal laser spikes.

Early work was done by Ready (16), who describes a phenomenological model of the vaporization step for a giant pulse laser. He showed that electrons are emitted from a graphite target in a manner that would be expected if a thermal rather than photoelectric process were involved. He also gave evidence indicating that as a result of the high pressures induced by the high photon flux of the laser, the heat of vaporization of the metal may approach zero.

Other experimental work on the target surface environment, during laser irradiation, was done by Archbold, Harper and Hughes (1). They indicated that the surface temperature of copper metal, when using a Q-switched laser, reaches 5000 °K, within 50 nsec. This would indicate, that with most Q-switched lasers, this temperature would be reached before the laser is off. It was also indicated, that temperatures as high as 10,000 °K might be reached in some cases.

Snetsinger and Keil (17) using a ruby laser of 0.4 J operated at 660 V above a 2200 V threshold, estimated the amount of material vaporized from the crater volume. Values of 0.5 μg or more were estimated. The laser output had three spikes with a 5 μsec time span.

The amount of material vaporized has also been measured by collecting it on the walls of a container. The material was dissolved and the concentration of the solution measured spectrochemically (22). The work was done with a normal laser, having an energy of 2.5 J. The amount of material vaporized was in the 0.X mg range. The investigators also gave evidence that with a copper target, as much as 80% of the energy from the laser beam could be lost by reflection. This value was obtained, assuming that a low-density plasma was formed during the laser pulse. The plasma is quite dense in Q-switched laser pulses (12).

Early work was also done by Archbold, Harper and Hughes (1). By using time-resolved spectra from plumes of various solid targets, they found a submicrosecond burst of continuum emission corresponding to each of a series of 1-MW laser spikes spaced a few microseconds apart. They apparently concluded that the continuum emission occurred at the surface of the target. They also gave evidence of both neutral and charged target species above the surface of the sample.

Indications that the laser beam energy may not all reach the target surface were given by Meyerand and Haught (11) and Tomlinson (14), who observed absorption of a focused laser beam by the plasma caused during gas breakdown. By placing detectors on the far side of the focal point, they reported that less than 10% of the light passed, depending on the shape of the laser pulse and power.

Further work with laser produced plasmas was done by Tomlinson (18). He used plasmas to control the shape of the pulse from the laser. If similar gas breakdown occurs at the target surface, laser produced plasmas could have great effects in limiting the amount of sample vaporized with increased laser power.

A theory concerning the process of absorption of laser energy by a plasma was given by Wright (21). He proposed that electrons absorb energy from many photons by inverse bremsstrahlung. Inverse bremsstrahlung refers to absorption of energy from photons by

the electrons of the plasma.

An intense continuum background was also observed by Minck (12). Measurements made of the electron density in the plasma varied from 5×10^{19} electrons/cm^3 for a discharge in air to 5×10^{17} electrons/cm^3 for a discharge in helium. These figures indicate the plasma is quite dense. Streak photographs of the luminous front permitted measurements of velocities of 10^7 cm/sec.

Piepmeier (15) has mapped the continuum emitting plasma and shown it to be cylindrical in shape rising in the direction of the laser beam. He also showed, that if the target was at an angle, the continuum was also in the direction of the reflected beam.

Gregg and Thomas (6) have indicated that the plume plasma temperature, when using beryllium targets in a vacuum, increases with a slope of 0.5 as a function of laser power. Temperatures as high as 8×10^5 °K were calculated using line intensities and by assuming black-body emission from the continuum-emitting plume.

Piepmeier (15) has shown from photodiode measurements, that the velocity of the continuum emission when using a ruby 8-MW, 50-nsec, Q-switched laser, is about 4×10^6 cm/sec. He also showed that the luminous-front velocity increases with laser power. This might indicate that increased energy is being absorbed by the plume plasma, and is used in forming a larger amount and volume of plasma.

Namba, Hyonkin and Itoh (14) using a 50-nsec, 6-MW neodymium laser and a tantalum target in a vacuum, have shown that ions of two energies are in the plume plasma. One of the energies of the ions increases linearly with laser intensity and can be considered thermal in origin. The other ions of higher energy increase at rate of $E^{1.5-2}$ as a function of laser intensity. These are considered as thermal ions which have gained energy from the electrons in the plasma.

It has also been indicated (8), that with increased power, the line emission increases, and with increased energy the amount of material vaporized increases.

Mandelstam, Pashinin, Prokhorov and Sukhodrev (10) have pointed out three stages in the interaction of the laser beam with the target material. The first is the breakdown of the gas by the electrons emitted from the target surface. The second is the stage of high electron density in the plasma resulting from energy absorption from the laser. The third is the afterglow period where the plasma is releasing its energy.

Piepmeier (15) has shown that the afterglow in air exists for only a few tenths of a microsecond.

From these investigations, it may be suggested that the amount of vaporized material should be somewhat independent of laser power due to absorption of the laser beam energy by the plume plasma.

Evidence in support of this hypothesis is demonstrated in the following experiments.

III. EXPERIMENTAL

A. Laser and Optical System

A Q-switched neodymium-doped glass laser was used in these experiments. The laser had a peak power of 3-10 MW, depending on the Q-switch and alignment conditions. It had a maximum repetition rate of one pulse every 10 sec. The average halfwidth of its light pulses was 50 nsec. The wavelength of the electromagnetic radiation is 1.06 μ. A sketch of the laser and its optical system is shown in Figure 1. The neodymium-doped glass rod is 14.5 cm long and 1.0 cm in diameter. The ends of the rod are cut at the Brewster angle. The coherent radiation coming from a laser cut at the Brewster angle is plane polarized. The EG&G FX-47B-6.5 Xenon flash lamp and the laser rod are water cooled. The inside of the ellipsoid reflector is plated with silver. The cavity is also purged with nitrogen to minimize ozone formation, which is damaging to the mirrored reflector. The quartz rotating prism and front sapphire resonant reflector are separated by 58 cm.

The power output could be best controlled by flashing the flash lamp once below threshold just prior to firing the laser. This aids in achieving thermal equilibrium in the rod.

A permanently mounted continuous Helium-Neon gas laser was used for alignment of the front reflector and rotating prism. The

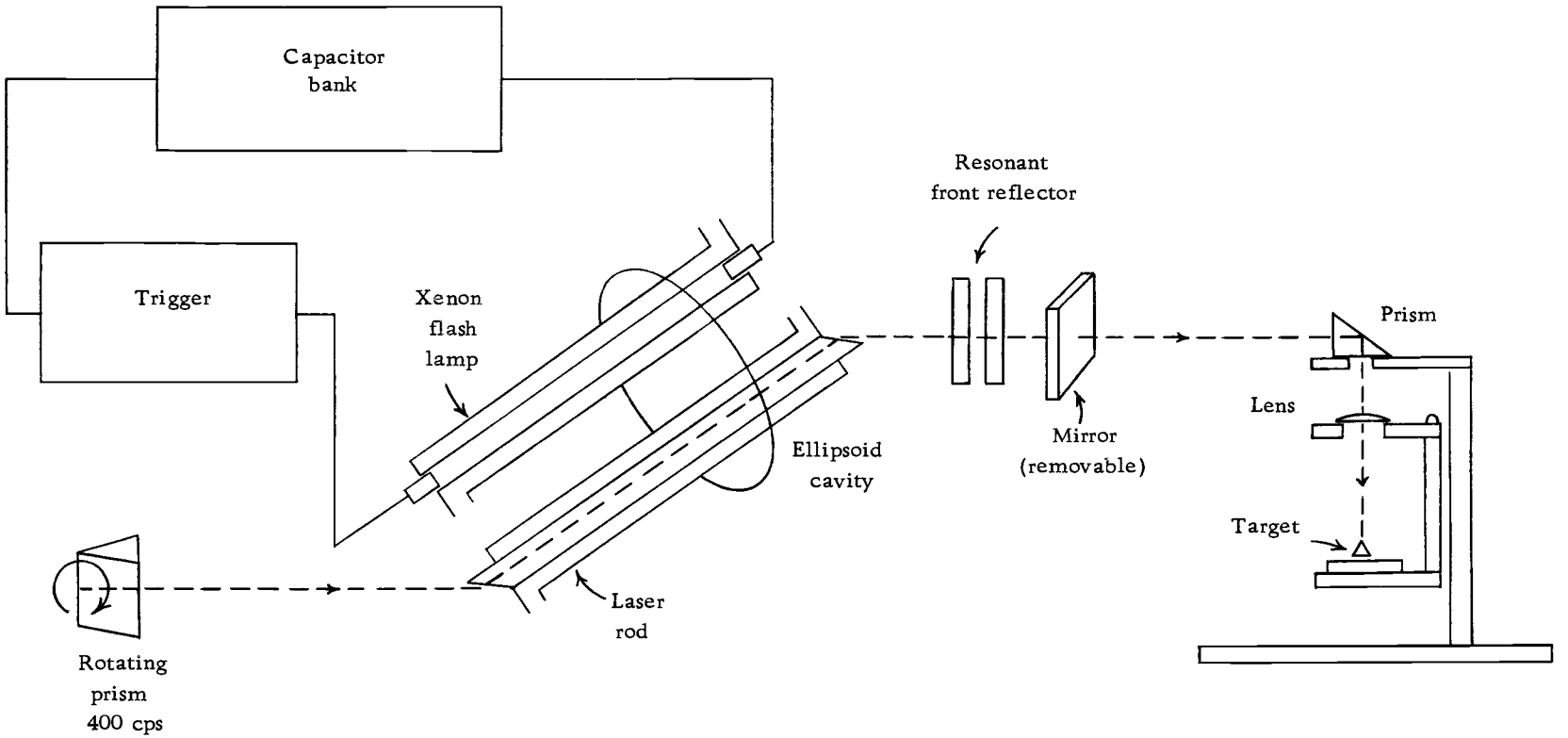

Figure 1. Laser and optical system.

beam from the gas laser was reflected into the optical path of the neodymium laser with a removable mirror. The mirror was removed before the neodymium laser was fired.

The laser beam was reflected 90 degrees with a glass prism and focused with a 38-mm focal length glass lens. The target was put at the focal point of the lens.

B. Measurement of Ejected Material

1. Experimental Apparatus

The experimental apparatus is shown in Figure 2. The laser beam is reflected 90 degrees with a glass prism, which is then focused with a glass lens having a focal length of 38 mm. The collecting vial is made of teflon, having an outside height of 40 mm and an inside depth of 38.1 mm. The vial is rod shaped, with an outside diameter of 35 mm and an inside diameter of 9.5 mm. The vial sits on an aluminum stand and its position is adjusted with four set screws, two of which are shown. The vial is held against the set screws with a rubber band. The lens is removable and is held in position with iron pins and sealed with clay. The 18 gauge copper wire sample target is positioned in the vial as shown and bent so the top surface is at the focal point. The wire target projects 0.1 mm above the bottom surface of the vial. The wire is held in position

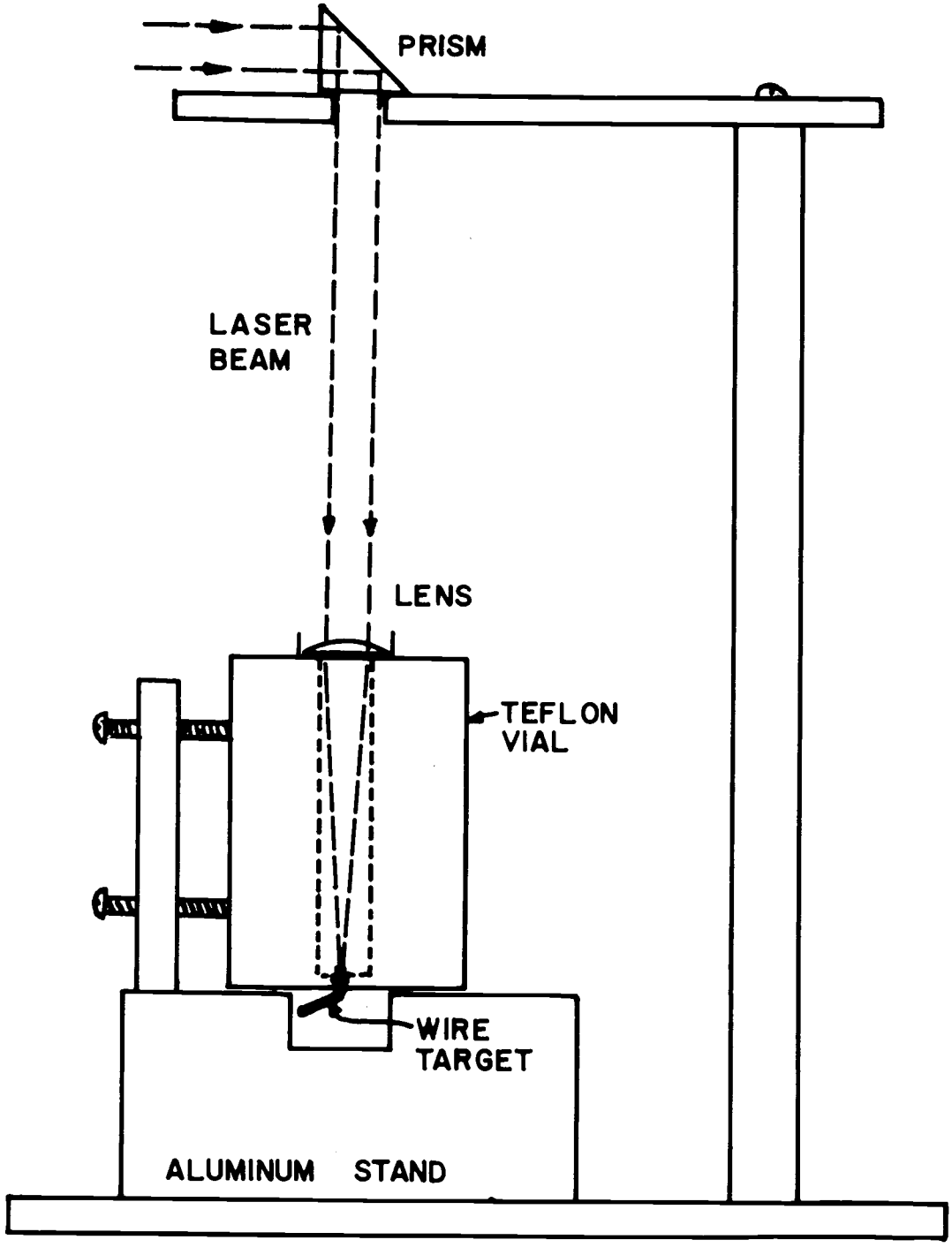

FIGURE 2. SIDE VIEW OF THE COLLECTING VIAL

with tape. The bottom aluminum stand was held firmly in place on a micrometer stand and could be easily removed for other experiments. The hole in the aluminum stand allowed the copper wire to project from the vial.

2. Alignment of the Wire Target

The laser beam was first centered on the front of the glass prism, which reflects the beam 90 degrees. The shape and position of the laser beam was determined by placing a piece of unexposed, but developed polaroid film, in front of the prism. Firing of the laser beam, knocked silver off the portions of the film where it was hit. The prism was then adjusted and the procedure continued until the glass prism was in proper position.

A rough alignment of the vial and sample target was then made by sighting as shown in Figure 3. The lens is centered below the prism by moving the aluminum stand.

The room lights were turned off for the fine alignment of the wire target. A flashlight was focused on the base of the teflon vial to light up the inside of the cavity. Sighting was made again as in Figure 3. The apparatus becomes a microscope when sighting in this fashion. The view seen in the front reflector of the laser at perfect alignment conditions, when sighting as before, is shown in Figure 4. The square shaded part is the shape of the prism with its

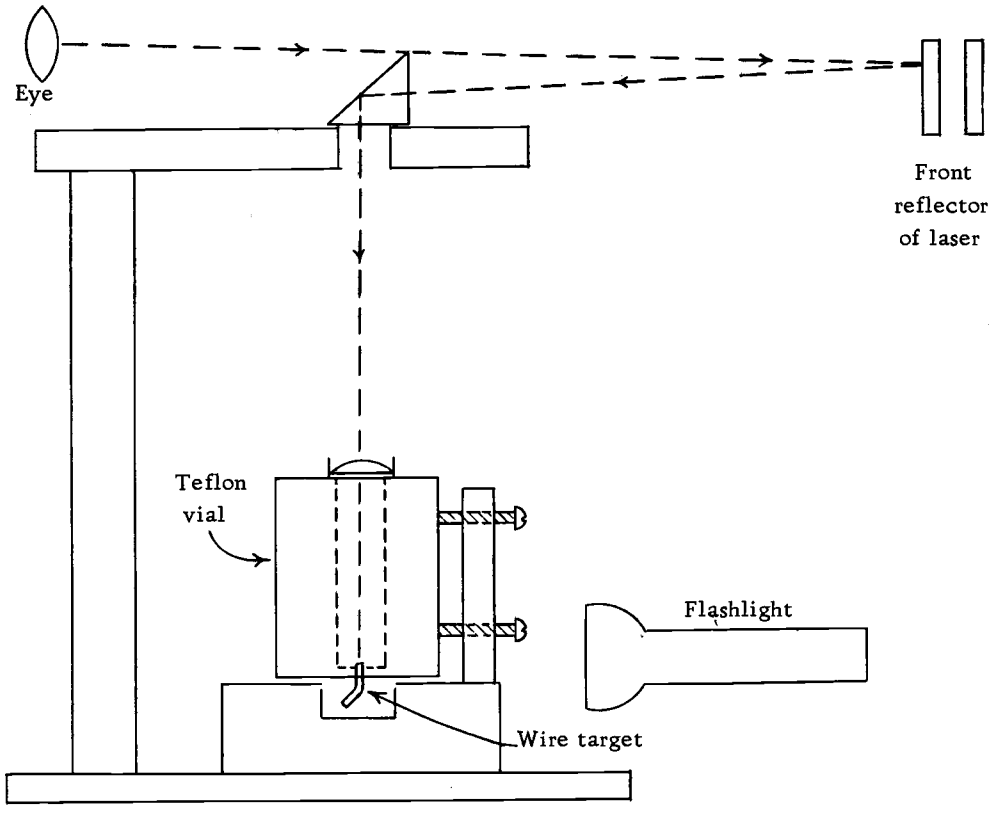

Figure 3. Sighting for alignment of wire target.

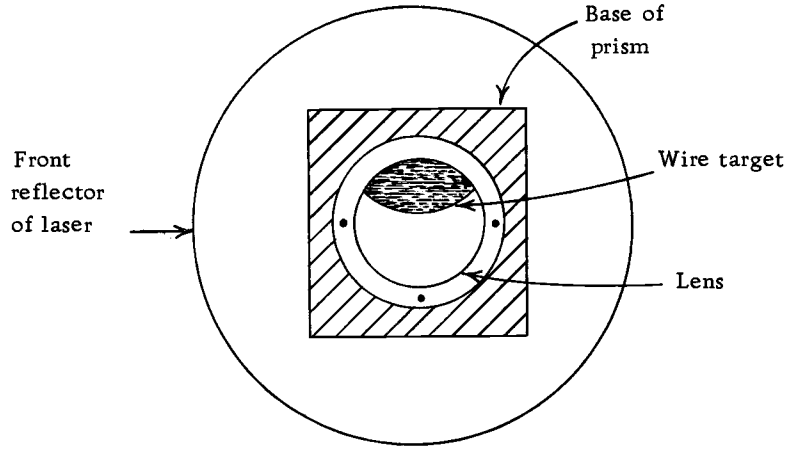

Figure 4. View in front reflector.

hole below it. The round concentric circle inside the prism hole is the lens on the teflon vial, with the three pins visible that hold the lens. When sighting in this fashion it is not possible to look through the back of the prism. As a result, it was necessary to set up criteria to estimate when the wire would be centered below the lens if one were sighting through the back of the prism. The dark part, in Figure 4, inside the lens is the portion of the wire that should show, when sighting as in Figure 3, in order to assure alignment. If one could then sight through the back of the prism the wire would cover the entire lens.

Diffraction patterns were noted along the edges of the wire target, when sighting in the above manner.

3. Sample Preparation

Each sample is made of 18-gauge pure copper wire, 4 cm in length. The wire is bent at a 90-degree angle, with the end filed flat, such that it was approximately the correct length to be at focus, when it was inserted into the teflon vial. The precise length was obtained by sanding the end of the wire with a fine emery cloth. This also gave a reproducible surface. The exact focal length of the lens, determined with a Ne-He gas laser, was used to determine the length of the bent portion. All samples were matched to a wire used as a model. The wire target was then washed with distilled water and

dried. The sample was never inserted into the vial until just before an experimental run.

The position of the wire can be seen in Figure 2. This only shows the part next to the teflon vial. The handle of the wire was about 38 mm long, for easy handling. The bent portion of the wire was 2 mm long with only a 0.1 mm of this bent section projecting inside the vial.

4. Measurement of the Collected Material

In each experimental run, the wire was hit with the laser beam five to ten times. In other experiments, runs were made using different wires for each of the shots. No detectable difference was found in the experimental results. The lens and the wire were removed 2 min after the last strike of the laser beam. This time was allowed, to let the vaporized material settle. Tape was then placed over the base hole in the teflon vial, and the glass lens was removed. This was followed by adding 0.50 ml of 30% by volume nitric acid from a 0.50 ml pipette through the top of the vial. The solution was then rolled around so that it would come into contact with the walls of the vial. The solution was allowed to stand in the teflon vial for 2-3 min, and was then transferred to a labeled container.

The analysis of the concentration of this solution was made by atomic absorption measurements. A Jarrell Ash atomic absorption

instrument, with a Sargent recorder was used in the analysis. The hollow cathode was used at 8 ma and was pulsed with a rotating disc. The copper line of 3247 A was used. A total consumption burner, using hydrogen and air, was used for atomization. The pressure settings for the hydrogen and air were 7 and 27 psi, respectively. A five-pass optical system was used with this instrument. The recorder, which had a variable sensitivity, was used at the 2-mV full scale setting. The lowest sensitivity, of 1-mV, was not used due to excess drift. In this mode, the recorder gave about 5 ppm sensitivity full scale. Typical recorder deflections with noise levels are shown in Figure 5. The deflections corresponding to the 0.6 ppm concentration are typical standards used in the calibration curve and also show the reproducibility of the instrument. The reproducibility was normally about ±0.04 ppm. The 0.2 ppm deflection is an example of the analysis of a solution taken from the teflon vial. Because of the rate at which the solution is sampled and the noise level, it can be seen from Figure 5 that 0.50 ml of solution is about the smallest amount of solution that can be used for accurate work with this method. A typical calibration curve is shown in Figure 6. The percent transmittance values are plotted on a logarithm scale to improve linearity. The analysis in these experiments was in the 85-100% transmittance region. The standards for the calibration curve were made with 30% nitric acid as the solvent, which is the same

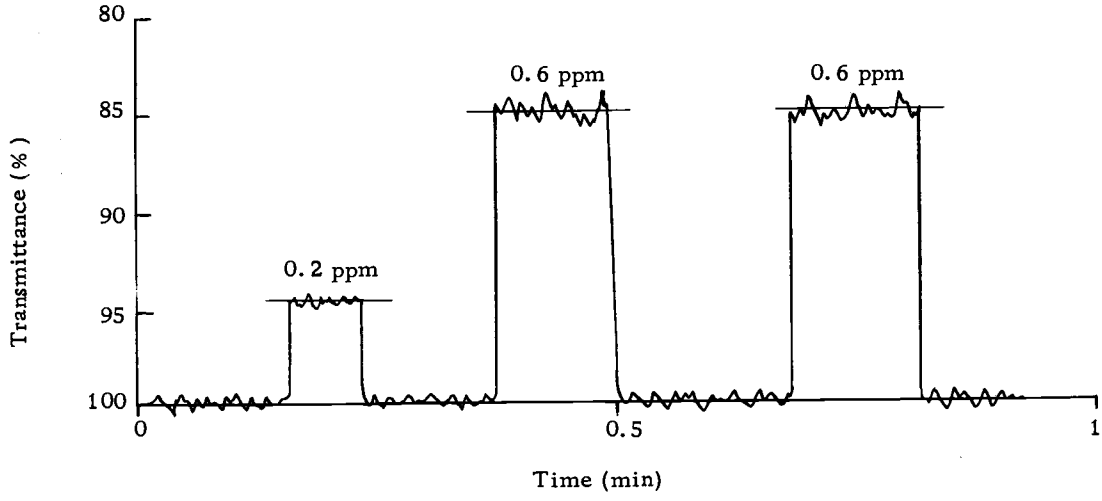

Figure 5. Typical readout on recorder chart paper.

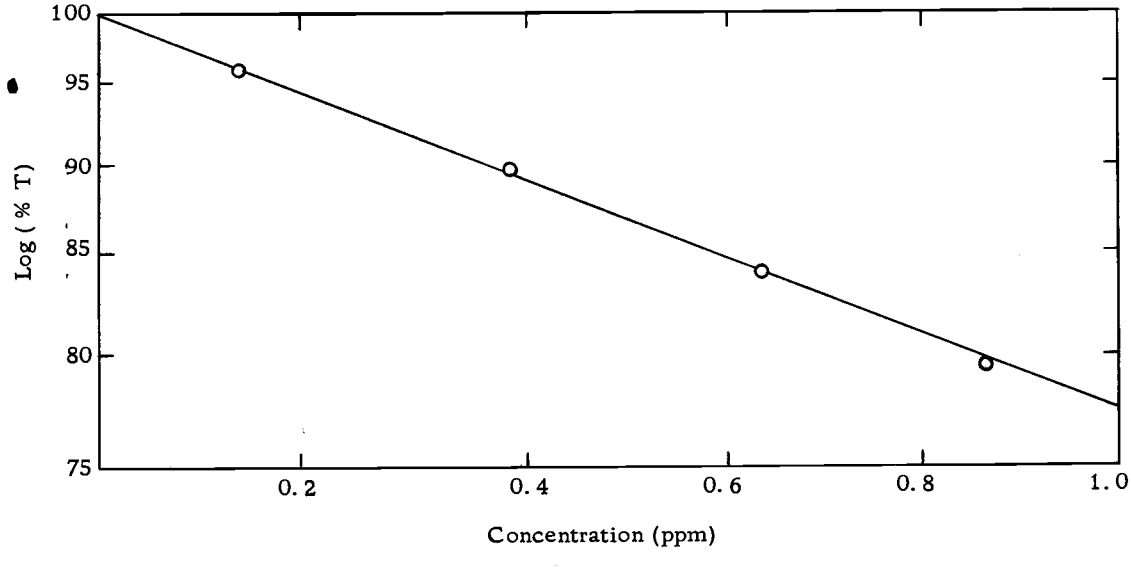

Figure 6. Typical calibration curve for atomic absorption.

acid solution that was used in dissolving the collected copper. By also using this solvent for a blank, the copper impurity level in the acid solution is no longer of concern, because the 100 % transmittance is set with this solution aspirating into the flame.

An analysis was made of the amount of copper that came off when the wire was inserted in the usual manner, but without firing the laser. It was found that no detectable amount came off. This is also a check on impurities coming from the tape.

Between runs, the teflon vial was cleaned by pouring the nitric acid solvent through it, followed by distilled water. The last acid solution that was poured through the vial was checked for copper impurities. The vial was then dried with Kimwipes and the lens and a new wire target were replaced for another experimental run.

From the concentration, in μg/ml, the total amount of copper ejected from the target was obtained. The amount ejected for each strike of the laser beam was obtained by dividing by the appropriate number of hits of the laser beam.

C. Laser Energy Monitoring System

1. Detection and Oscilloscope Triggering

The top view of the laser energy detection system is shown in Figure 7. The laser beam first goes through a removable liquid-absorbing cell. This cell was filled with copper sulfate solution,

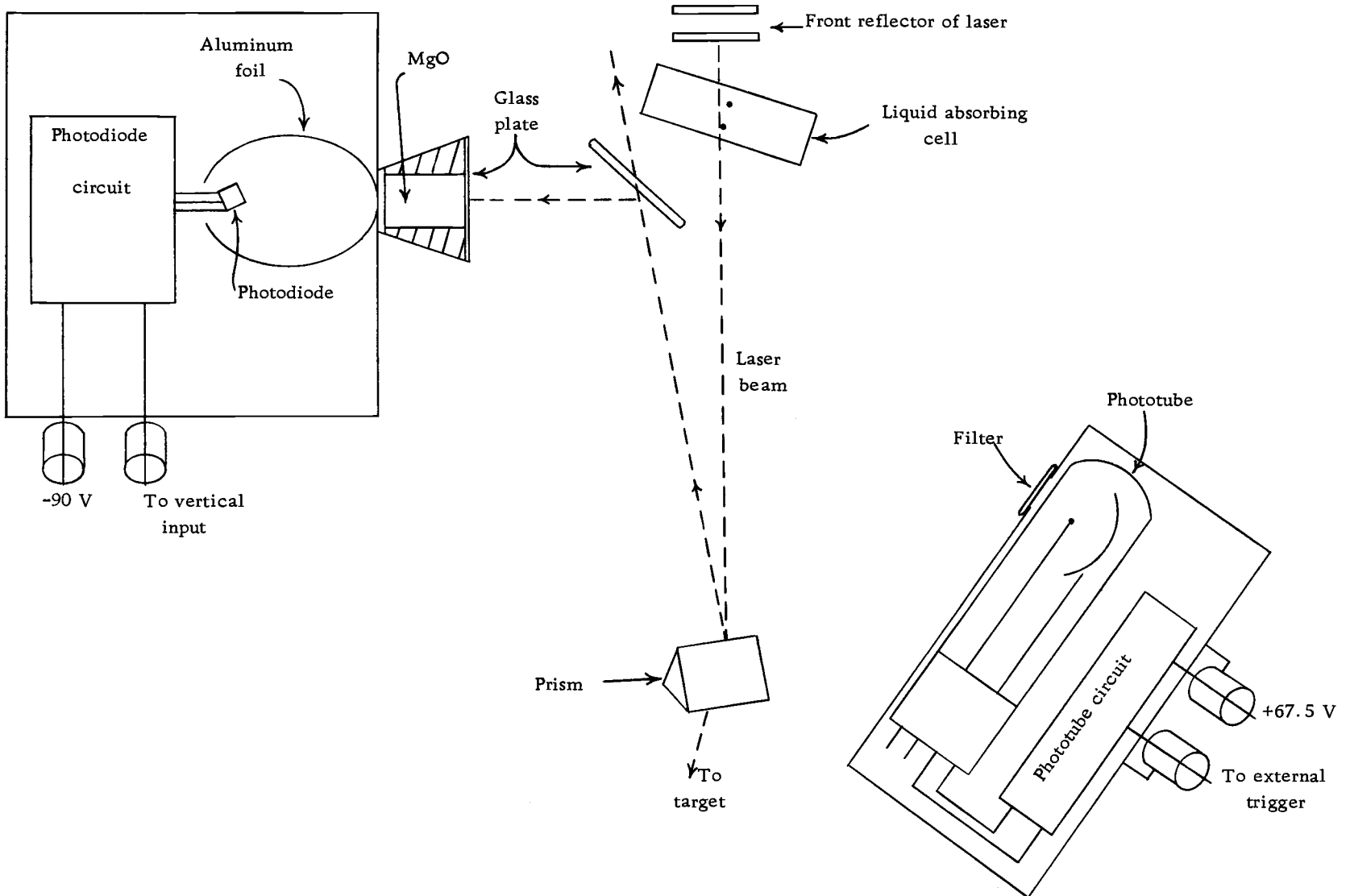

Figure 7. Top view of energy monitoring system.

with concentrations varying from 5×10^{-1} to 5×10^{-3} M, which absorbs in the wavelength region of the laser beam. In order not to reflect light directly back into the laser, the cell is at a slight angle. After the radiation has gone through the absorbing cell, it strikes the glass prism, which reflects the beam down to the target. A fraction of the light that reaches the prism is reflected off the front surface. This reflected beam goes to a glass plate, where most of the radiation goes through. Again a fraction of the beam is reflected. The light beam is then diffused by going through a 1-cm thickness of magnesium oxide powder. Only a 3-mm thick layer of the powder was used at low laser beam energy. The diffuse radiation then enters a reflecting cavity made of aluminum foil. The diffuse light is then detected by an SGD-100 photodiode, which sends a negative voltage signal to the vertical input of a Type 141 dual-trace plug in unit of a 555 Tektronix oscilloscope. This oscilloscope has a rise time of 15 nsec. The electronics of this system will be discussed in the next section.

The oscilloscope triggering system is also shown in block form in Figure 7. Stray laser light and radiation from the plume is collected on the cathode of a phototube. Blue-colored paper was put over the entrance to the phototube in order to reduce room light reaching the cathode. The triggering system sends a large positive voltage signal to the external trigger of a type 22A time base unit,

in a Tektronix oscilloscope. This separate triggering unit was included in the system, due to difficulty in triggering off the photodiode signal. The sweep time of the oscilloscope was set at 0.2 μsec/cm.

2. Electronics and Readout

Circuit diagrams of the phototube and photodiode systems are shown in Figure 8. The photodiode is a reverse biased diode which is sensitive to light. A 1-μF capacitor is put in parallel with the battery to by-pass the signal around it. With no light present, the photodiode is a high resistance and little current flows. When light strikes the photodiode, charge carriers are produced and the increased current flow develops a negative voltage across a 53 ohm load resistor. A RG58/v coaxial cable, with a characteristic impedence of 53 ohms was used to carry the signal to the oscilloscope. The cable was properly terminated to prevent reflection. Typical voltage pulses were 5-50 mV.

The phototube circuit is also shown in Figure 8. It is similar to that of the photodiode. When no light hits the phototube, little current flows. However, when light from the laser and plume strike the cathode of the phototube, electrons are ejected and the resulting current causes a voltage signal of about 2 V to appear across a 10,000 Ω resistor. Coaxial cable was used to carry the

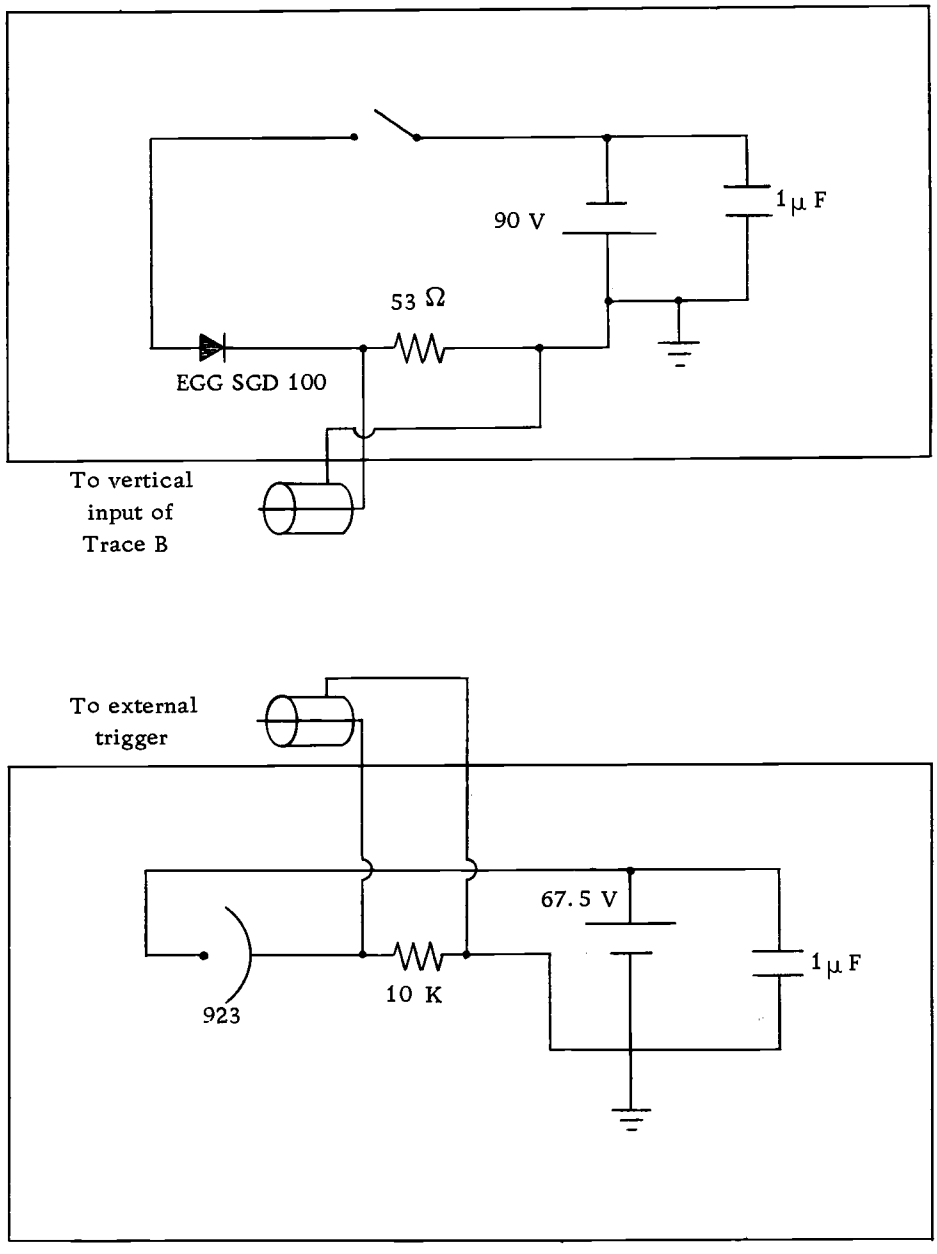

Figure 8. Circuit diagram of the energy monitoring system.

signal to the external trigger of the oscilloscope. The phototube was used because of its fast rise time, but was not used for monitoring the laser beam, because of its slow fall time.

The trace on the oscilloscope was photographed with high speed Type 410 Polaroid film. A drawing of a typical picture of the trace is shown in Figure 9. The negative voltage pulse from the diode circuit appears on the trace, as shown by the arrow.

3. Calibration with Calorimeter

The photodiode monitoring system was calibrated with a calorimeter. The calorimeter was insulated with styrofoam, and placed below the glass prism to match as closely as possible the optical environment of the target material. The laser beam entered the calorimeter and was absorbed by a copper sulfate solution. The resulting temperature rise, was measured by a thermistor and recorded on a Heath recorder (15). The readout of the calorimeter on a Heath recorder is shown in Figure 11. When the laser beam hits the calorimeter, the temperature rises quickly. Because the system comes to equilibrium slowly, it is necessary to extrapolate the exponential cooling curve to zero time. The temperature rise at zero time is shown by the arrows. The temperature rise is related to the laser beam energy by the heat capacity of the calorimeter. The recorder was calibrated by switching calibrated resistances into the

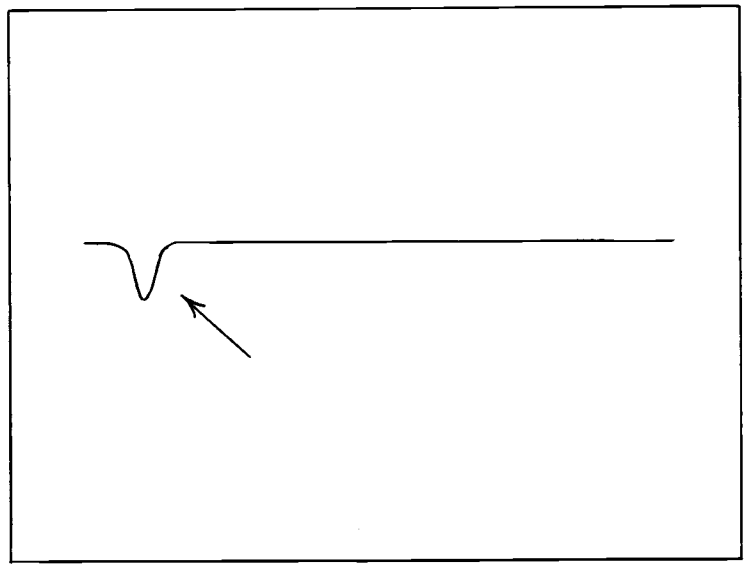

Figure 9. Laser energy readout.

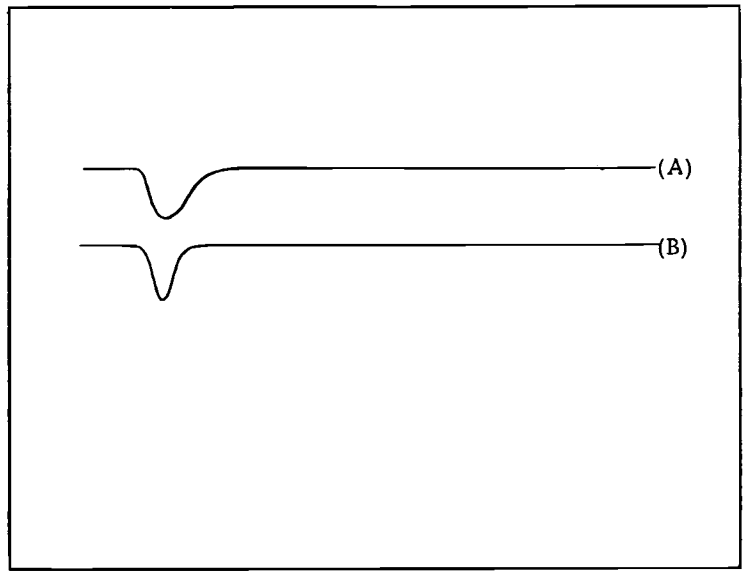

Figure 10. Plume continuum and laser energy readout.

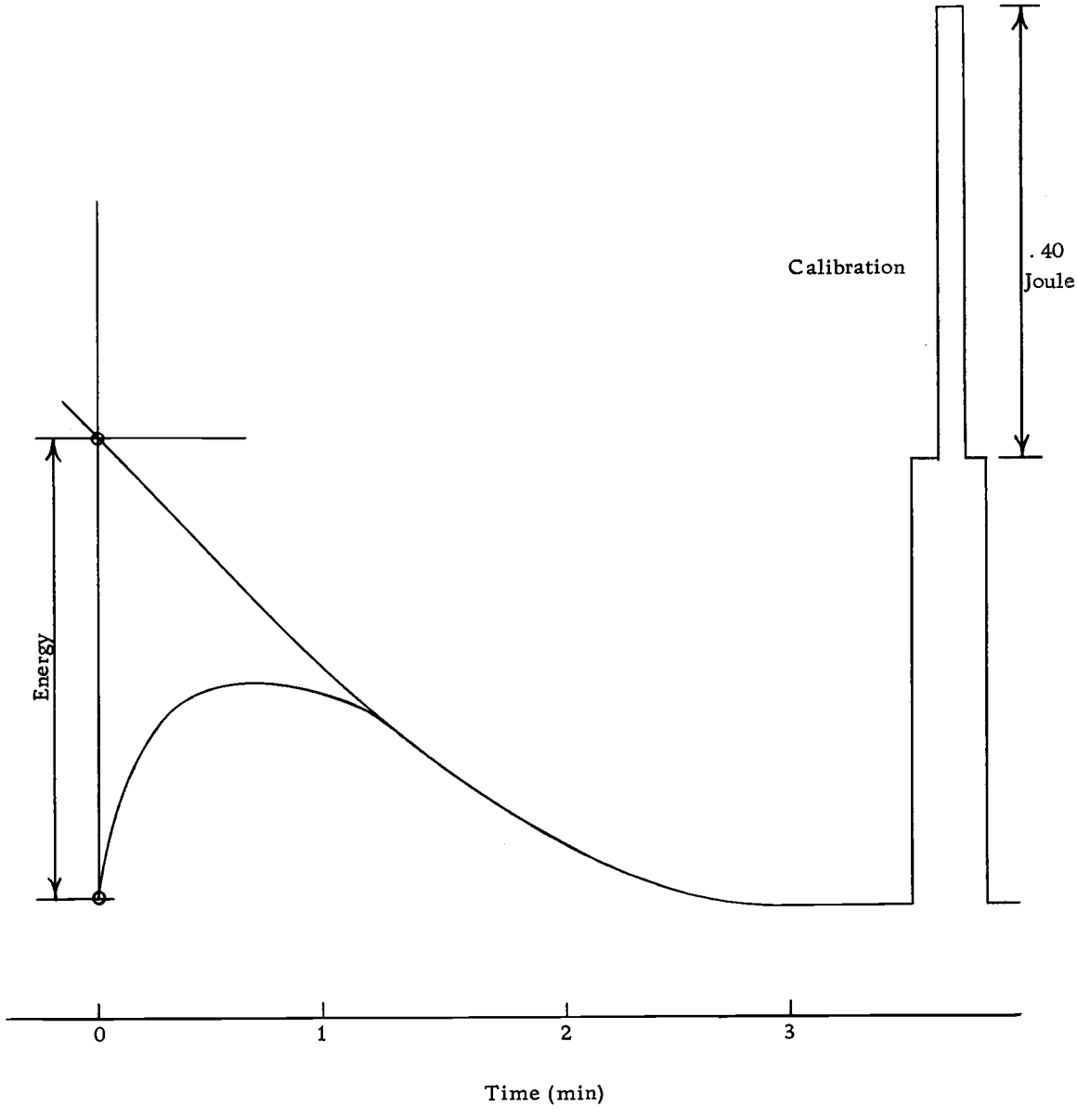

Figure 11. Calorimeter readout with Heath recorder.

circuit of the calorimeter (15). In this manner, the laser beam energy can be directly related to the number of divisions on the chart paper at the extrapolated zero time.

Calibration curves of the photodiode monitoring system were made by measuring the area under the oscilloscope trace and graphing it versus the energy of the laser beam as measured by the calorimeter. The area under the trace was obtained by multiplying the half width by the height. As the photon flux, or laser beam power increases, the oscilloscope deflection also increases. Because energy is the integral of power with time, the area under the oscilloscope trace is proportional to the energy of the laser beam. Typical calibration curves are shown in Figure 12. Curves were made for several voltage sensitivity settings on the oscilloscope. This enables one to get area measurements with a relative precision of ±7%, over a large range of laser beam energies. As can be seen, the curves are quite linear. Typical uncertainties are shown on the plot.

D. Control of Laser Energy

In the normal mode of operation, the laser was fired with a flash lamp voltage such that it is just above threshold conditions. This varies with alignment and optical condition of the rotating prism. When the laser is fired in this fashion, the energy output

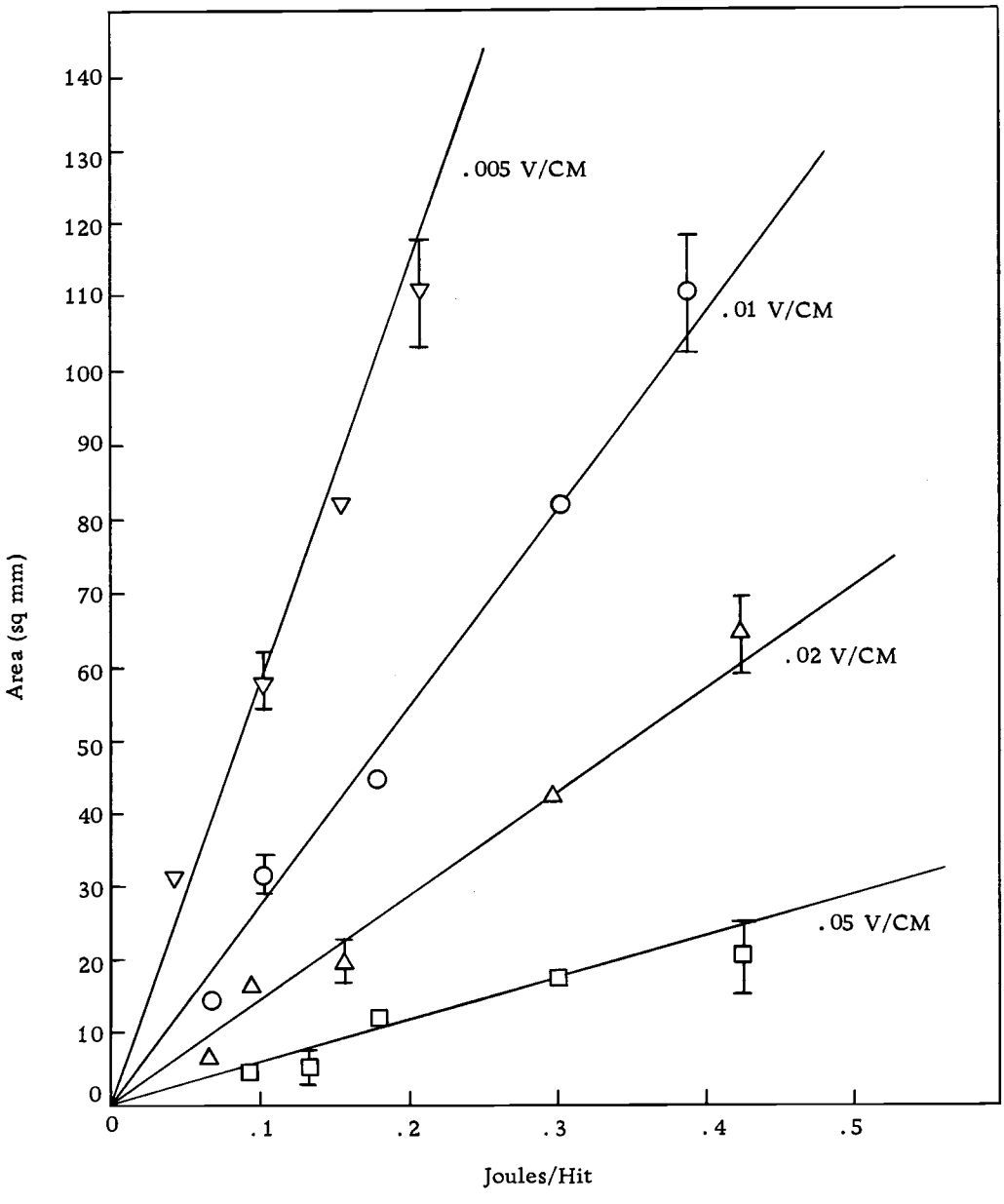

Figure 12. Calibration curve of photodiode.

is about 0.15-0.2 J. This energy corresponds to a power level of 3-4 MW with a 50-nsec halfwidth. If the laser rod is warmed up by first flashing the flash lamp below threshold, the energy output can be controlled within ±0.02 J in this energy region.

Higher energies were obtained by increasing the voltage on the flash lamp capacitor bank. Light pulses from the laser up to 10 MW and 0.5 J were obtained in this manner, when the rotating prism was in good condition. The maximum power levels used in the experimental work were 6-7 MW corresponding to an energy of 0.3-0.35 J. In this range, the energy could be controlled within ±0.03 J in the manner described earlier.

Low energy light pulses were obtained by using a 1-cm thick absorbing cell filled with copper sulfate solution. Concentrations varying from 5×10^{-3} to 5×10^{-1} M were used. This solution absorbs light in a wavelength region corresponding to that of the laser's radiation. Energy control within ±0.01-0.005 J was obtained in this low energy region.

E. Plume Continuum Measuring System

The relative continuum emission of the plume plasma was measured with the setup shown in Figure 13. The plume plasma gives off electromagnetic radiation similar to black-body emission.

Copper foil was used as the target material. The surface

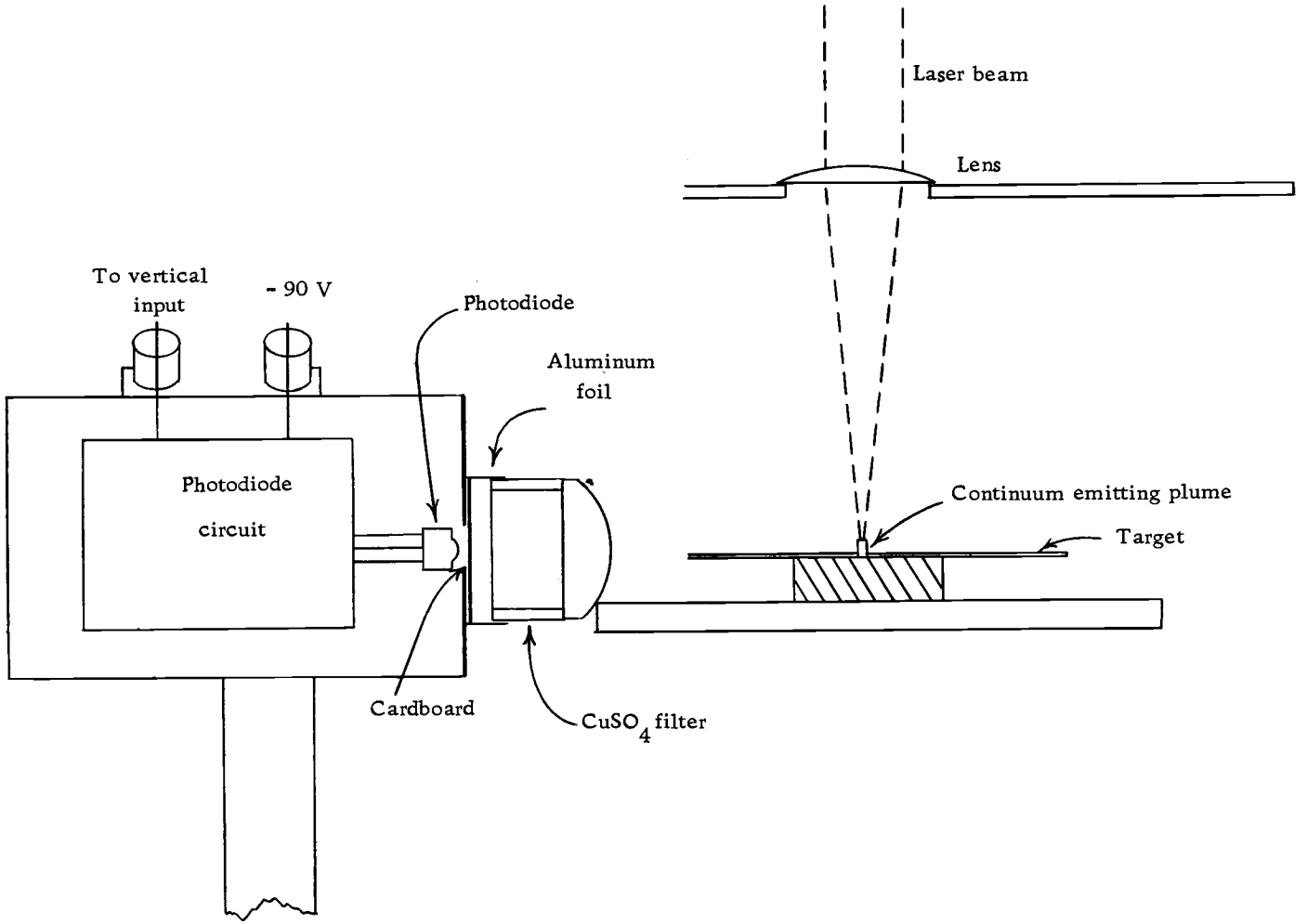

Figure 13. Plume continuum emission measuring system.

was prepared by sanding with fine emery cloth.

The continuum emission was measured with a photodiode. The circuit for the photodiode is the same as the one previously described. A 1-cm thick cell containing 1 M copper sulfate solution, was placed in front of the photodiode to absorb stray radiation from the laser. The front surface of the cell was a lens used in focusing the radiation from the plume plasma on the photodiode. The focal length of the lens was 58 mm. The photodiode was 35 mm from the lens. A piece of white cardboard was put in back of the cell to diffuse the light. Aluminum foil was placed around the cell to assure that no stray radiation from the laser was able to get to the photodiode. From the photodiode circuit, a negative voltage pulse was sent to the vertical input for trace A in the double beam Tektronix oscilloscope, while the signal from the laser beam monitor was sent to the B trace.

The same triggering system is used here as previously described. The only difference is, that trace A and B trigger on the same horizontal time base.

In this manner, it is possible to get measurements of the laser beam energy and the relative continuum emission of the plume plasma simultaneously. The area under the oscilloscope trace was used as a measure of the relative continuum emission of the plume plasma. The area was measured in square millimeters, by multiplying the

halfwidth by the height. The relative precision of the area measurements, went from ±10% to ±5% with increasing area over the range investigated.

The oscilloscope trace was photographed with high speed Type 410 Polaroid film, as before. A drawing of a picture of both the laser beam energy pulse and the relative continuum emission from the plume is shown in Figure 10 on page 25. Trace A is from the plume and trace B is from the laser beam.

IV. RESULTS AND DISCUSSION

A. Introduction

The experimental results together with a discussion of their meaning and analytical significance are presented in this section. A semiquantitative relationship between the energy transferred to the plume plasma and the continuum emission will also be illustrated. Finally, a theoretical model of the energy distribution will be proposed. This model is based on the author's experimental results, as well as those of others.

B. Quantity of Material Vaporized

Measurements, as described in Section III-B, were made of the amount of copper vaporized completely off of the target material. These measurements were made at different laser beam energies and powers. Both the energy and power were varied with liquid absorbers and flash lamp voltage, as described in Section III-D. The graph of the results is given in Figure 14. In each run, the target was hit by the laser beam five to ten times. The amount of material vaporized, was determined by dividing by the appropriate number of hits. Because it was possible to control the energy of the laser beam within ±10%, from one strike to the next, the energy of the laser pulses and the amount of material vaporized was

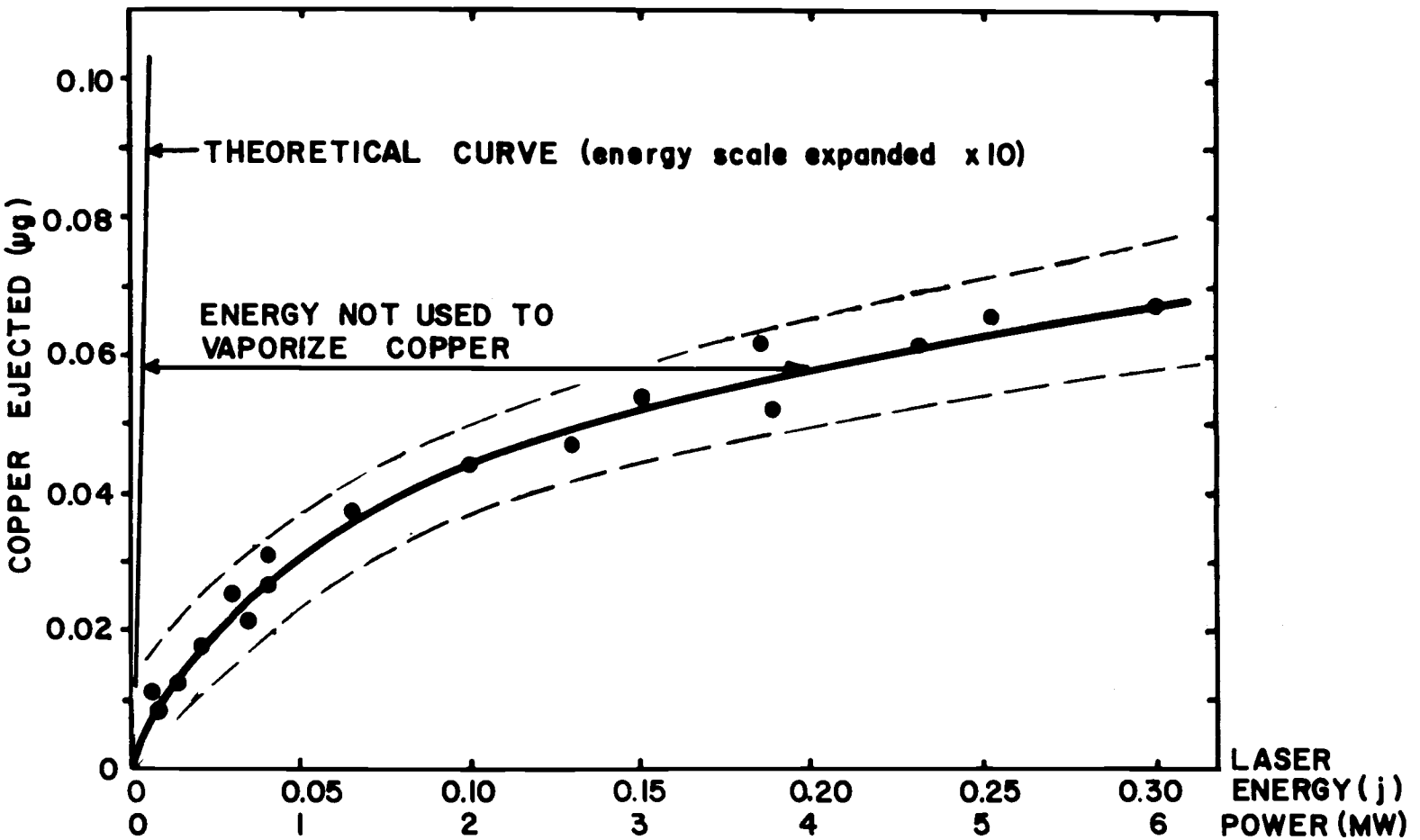

FIGURE 14. AMOUNT OF COPPER EJECTED BY A LASER PULSE

averaged assuming linearity over each small section of the curve. The laser beam peak power values are also included in Figure 14. These were obtained, by dividing the energy of the laser pulse by the average halfwidth time of 50 nsec. The halfwidth varied ±5 nsec. Plotting the function taking into account these small and random changes in the halfwidth did not change the shape or magnitude of the plot within experimental uncertainty. As a result, the function is graphed together with its uncertainties using a power axis calculated from the energy values and an average halfwidth. The uncertainties are shown with dashed lines. These were obtained from the precision of each of the measurements described in the experimental section.

As can be seen, the amount of material that is sampled and leaves the target is small, and therefore when used for analytical purposes on large homogeneous samples, it can be considered essentially nondestructive analysis.

The volume of material vaporized was compared with that measured by collection. These measurements were made under a microscope. It is difficult to get accurate measurements of the depth, due to the uneven floor of the crater and also the edges formed around it. A cross-section sketch of the crater formed by the laser beam is shown in Figure 15. This sketch was drawn, transposing from a top view seen through a microscope. The volume was found

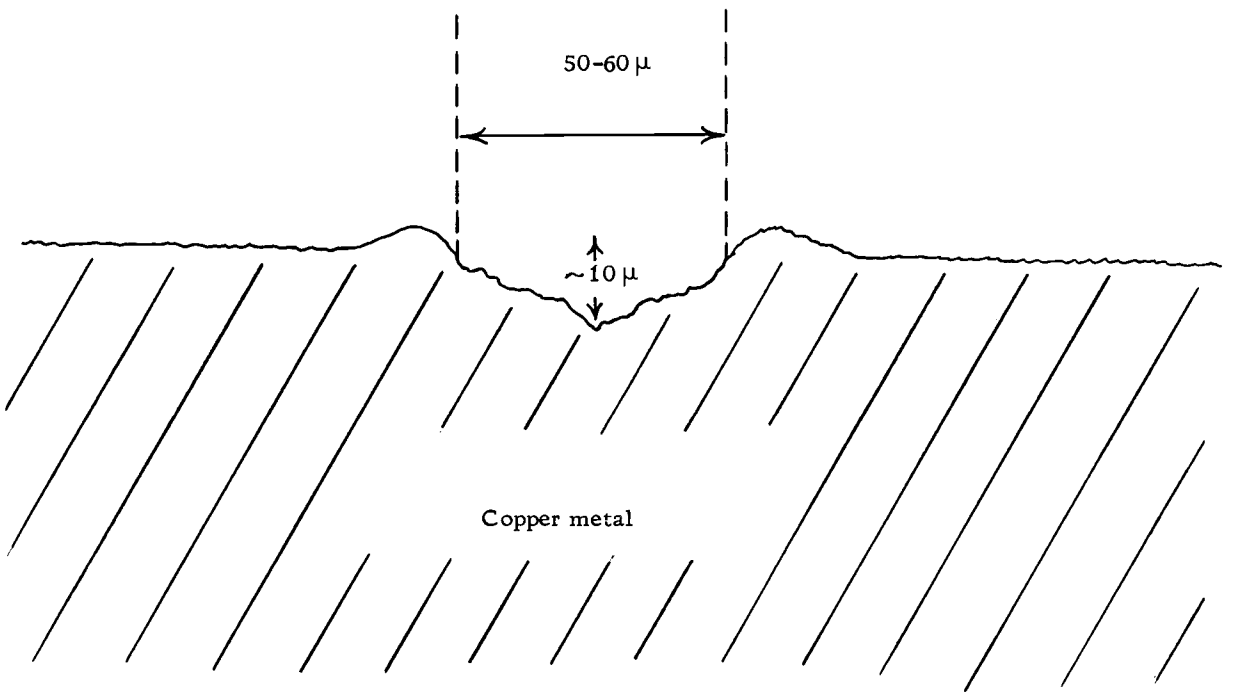

Figure 15. Cross section sketch of crater.

to be approximately 10^{-8} cm^3. The density of copper being about 9 g/cm^3, gives an estimated amount of vaporized material of 0.09 μg per hit. Because of the uncertainties of this measurement, it is of order of magnitude quality at best. It is however, in the same order of magnitude as the collected material measurements.

Theoretical estimates of the amounts of energy necessary to vaporize these small amounts of material, can be made with information available on the surface conditions of the target during the time the laser is on. Theoretical estimates and indirect measurements (1), have been made of the surface temperature of the target material during the time the laser is striking the target. Estimates of the surface temperatures for different materials, have ranged from 5000-10,000 °K, with a figure of 5000 °K given to copper metal. The normal boiling point of copper is 1300 °C. These temperatures might indicate, that of the energy that does reach the target, much may be used in ionization, excitation, and kinetic energy of atoms and electrons, or conducted away in the metal, rather than being used for vaporization. Assuming that the surface temperature is constant at all laser energies investigated, a curve can be drawn of the amount of material vaporized as a function of laser energy. This assumption, as will be seen later, does not have to hold completely to illustrate the point to be made. The plot of this calculated value is shown in Figure 14 for a surface temperature of 10,000 °K. This

plot was calculated using a constant specific heat for copper of 0.1 cal/g °K. The value for the specific heat was taken from handbook data at a temperature of 800 °C. No handbook data on specific heat was found above this temperature, so the value was assumed to be approximately correct for all temperatures up to 10,000 °K. Pressure effects on this value were also not available. Work done by Ready (16) has shown that with the high pressures at the target surface, during the time the laser is on, the heat of vaporization may approach zero. He also gave evidence, that the target material may go directly from a solid to vapor. The heat of vaporization was therefore neglected in the calculation. The amount of material vaporized completely off the target was taken from the experimental data. Below is a sample calculation for 0.05 μg of ejected material:

$$(0.1 \text{ cal}/^\circ\text{K g})(10^4\ ^\circ\text{K})(5 \times 10^{-8} \text{ g})(4.18 \text{ J/cal}) = 0.0002 \text{ J}$$

As can be seen, less than 1% of the available 0.15 J of laser energy is used in heating up and vaporizing the material that is completely lost to the target, assuming the above mentioned target conditions. The rest of the laser beam energy, must be lost by conduction, given to the plume plasma, lost by reflection, or used in vaporizing and heating material that recondenses on the surface of the target.

It can also be seen from the graph in Figure 14, that the amount

of material that is vaporized away, is not linear with laser energy and power. As the laser energy increases, the amount of material vaporized increases at a lower and lower rate. This indicates that a smaller fraction of the total laser energy is reaching the target at higher powers. As will be explained later, this is probably due to the greater absorption efficiency of the larger laser pulses, by the plasma formed above the target, during the laser pulse.

C. Continuum Emission

Experimental measurements were made of the relative continuum emission of the plume plasma as a function of laser energy and power. The experimental setup and procedure is discussed in section III-E. The plume mapped by Piepmeier (15), was shown to be cylindrical in shape rising in the direction of the laser beam.

The photodiode response was mainly governed by the continuum emission, rather than line emission of the target species. The poor response to the line emission results first, because the strongest copper lines at 3247 A and 3274 A are in a low spectral response region for this photodiode. Spectral evidence has also shown that the continuum emission is quite intense compared to the emission lines, while the laser is on (15). The emission lines normally continue for several microseconds after the laser is off (1, 15). Because the photodiode pulses lasted less than a microsecond, it is

evident that a negligible amount of the photodiode readout results from line emission of the target species.

The experimental results are shown graphically in Figure 16. The uncertainties in the measurements are also shown with dashed lines. As can be seen from the experimental measurements, the background continuum emission increases linearly within experimental uncertainty as a function of laser power. This linear increase in continuum emission indicates, that additional amounts of energy are being given to the plume plasma as the laser power increases. The linear increase in continuum emission also indicates that unless the spectral line intensity increases at the same rate, the line to background ratio will decrease in the spectrographic analysis of the target material. If the laser is to be used for vaporizing material for atomic absorption analysis, this higher continuum intensity will also cause background problems.

D. Relationship Between Continuum Emission and Plume Energy

Photodiode measurements of the continuum emission are approximately, but not rigorously, directly proportional to the energy transferred to the plume plasma. The basis of the relationship will be illustrated below, by showing that the photodiode responds to the temperature and the amount of plasma simultaneously.

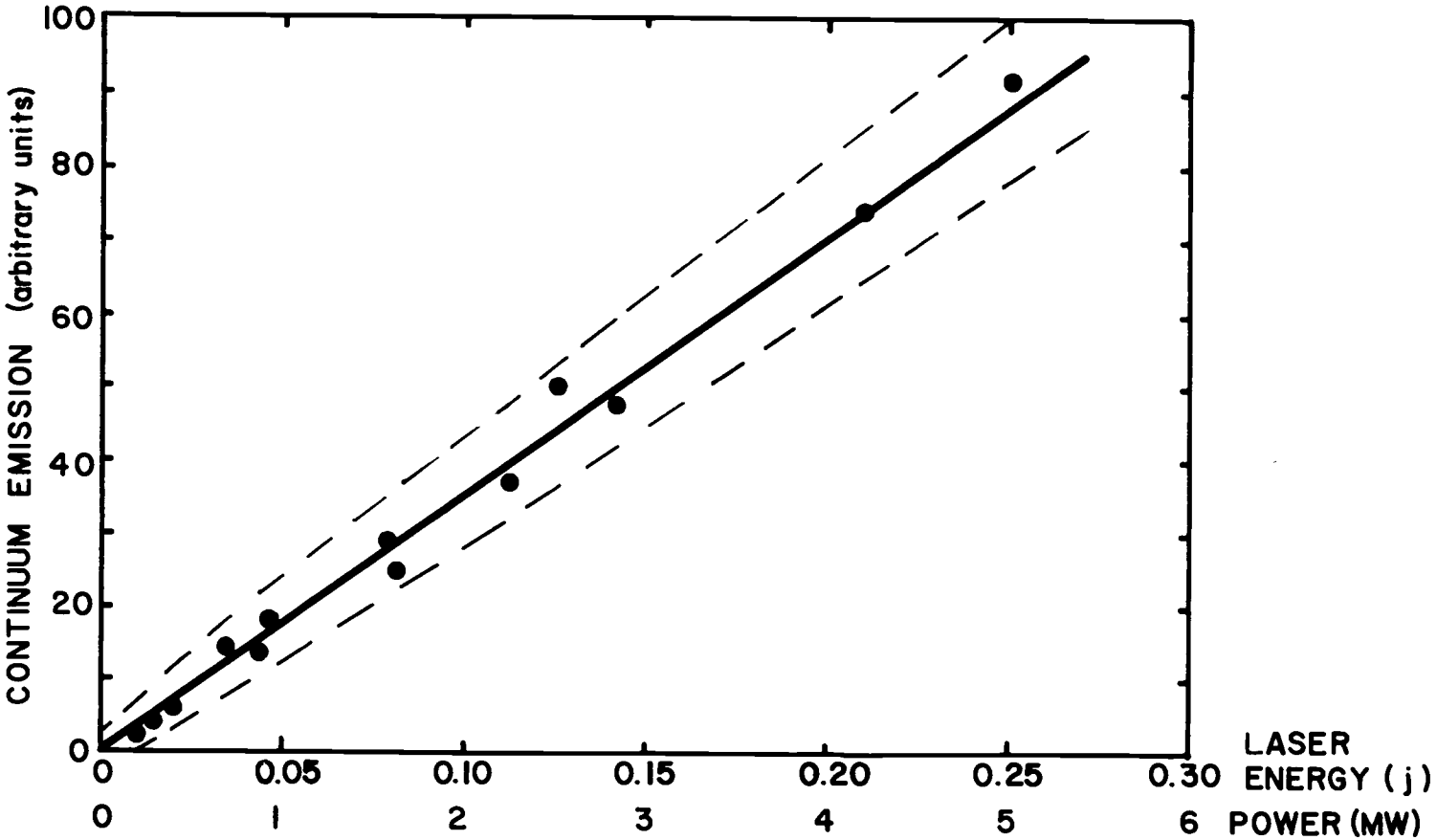

FIGURE 16. RELATIVE CONTINUUM EMISSION FROM PLUME vs LASER POWER AND ENERGY

The photodiode response is proportional to the temperature of the plasma, if the temperature is related to black-body emisson through Planck's black-body equation. Plasma continuum emission is approximately black-body emission (4, 6, 7). This approach to temperature measurement is valid only in high density plasmas (7), however plasmas formed above the target surface have been shown to be quite dense (12). Assuming black-body emission, the intensity of electromagnetic radiation in the spectral region of 3500-5500 A seen by the photodiode using a copper sulfate filter, is approximately linearly proportional to the temperature of the plume plasma in the temperature range of 5000-15,000°K (3, 6). This relationship is approximately valid, because the relative shapes of the black-body spectral intensity curves remain approximately the same over this temperature and wavelength range (3, 6). As a result, the photodiode response is approximately linearly related to temperature rise.

The photodiode response is also proportional to the amount of plasma. Because the diameter of the plasma is approximately defined by the diameter of the laser beam and remains approximately constant (15), the volume of the plume plasma is proportional to the height of the plume above the target. As a result, the emitting surface and therefore the emission seen by the photodiode is directly proportional to the volume. The volume of the plasma is directly related to the amount of the plasma. Since there is little horizontal expansion of the plasma during the time the laser is on (15), it is

reasonable to assume that there is little volume increase due to expansion until after the laser is off. Work has shown that the height of the plasma increases during the time the laser is on (15). The increased height and resulting increase in volume, together with the small expansion of the plasma, indicate that the increased volume of the plasma results from plasma formation, rather than plasma expansion, during the time the laser is on. As a result, it can be assumed that the amount of plasma is approximately proportional to the plasma volume. As was previously described, the volume of the plasma is proportional to the emitting surface and emission seen by the photodiode. Therefore, the amount of plasma is proportional to the emission seen by the photodiode.

The relationship between energy content and the product of temperature and amount of plasma is approximately linear (2, 20). Because the photodiode simultaneously responds to the temperature and amount of plasma in an approximate linear manner, the photodiode readout is approximately linearly proportional to the average plume plasma energy content. As a result, the greater the total amount of emission seen by the photodiode, the greater the total amount of energy transferred to the plume plasma.

As a result of this relationship, the graph in Figure 16 shows an approximate relative measurement of the energy transferred to the plume as a function of laser power. As can be seen from the

plot, the total energy given to the plume increases linearly as a function of laser power within experimental uncertainty. This energy might otherwise have been used for vaporizing sample material.

E. Energy Not Accounted For by Vaporized Material

The energy not accounted for by the vaporized material is shown graphically in Figure 17. This plot has been calculated, by subtracting the small amount of energy necessary to raise the temperature of the measured amount of copper vaporized to 10,000 °K, from the total laser energy. It was assumed that the temperature of the target material was constant at the laser beam powers investigated. However, because of the small energies needed for heating compared to the energy available in the laser beam, even if the target material did not have a constant temperature for different laser powers, the plot in Figure 17 would be approximately linear within experimental uncertainty. The energy difference that has not yet been experimentally accounted for, could result from energy transferred to the plume plasma, vaporization of copper that never left the target permanently, and energy lost by reflection and conduction.

Energy that could be accounted for by material that never left the target permanently, would account only for a small amount of the total energy available. It is difficult to conceive of energy losses in this way of more than 0.002 J, even if this material were raised to a

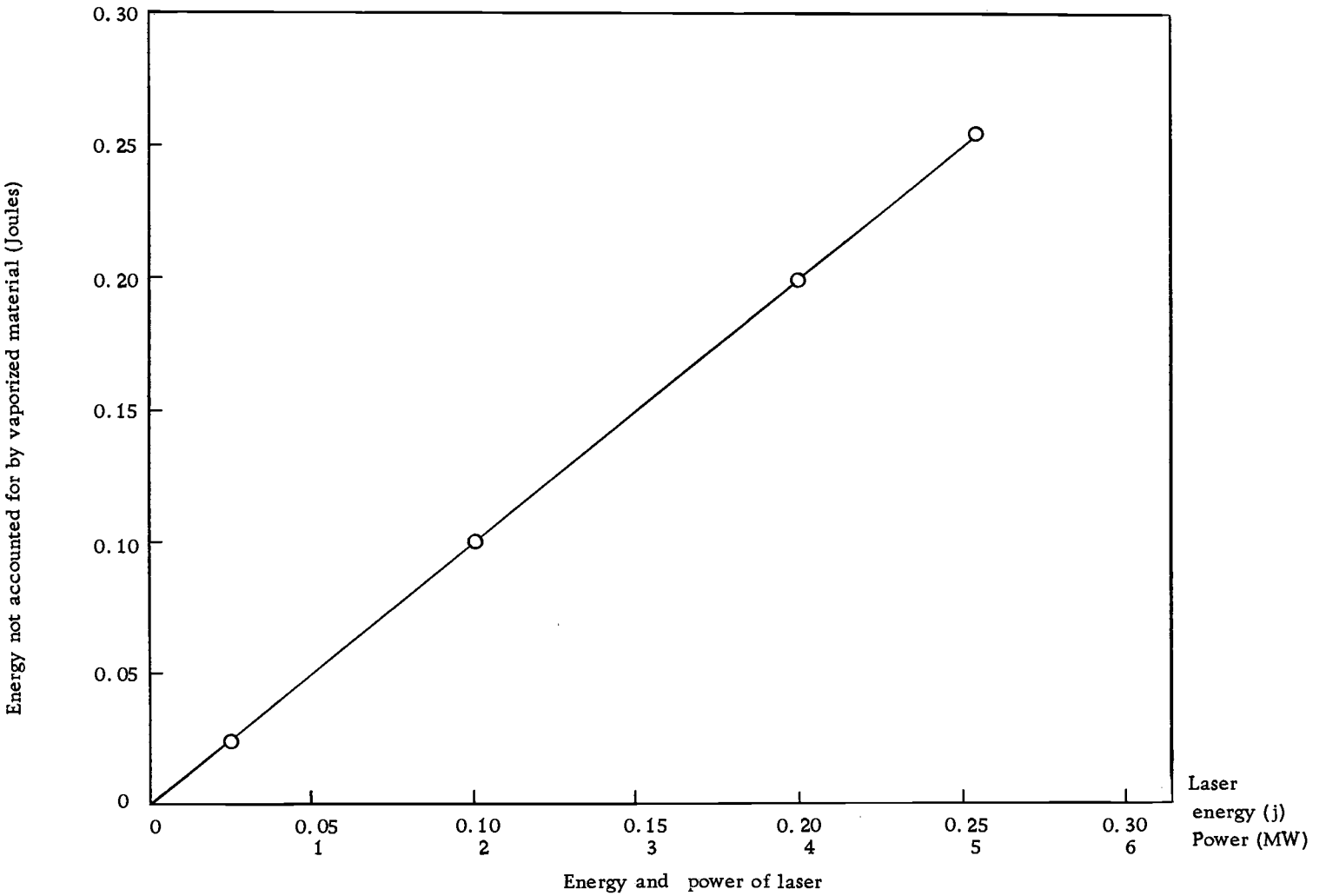

Figure 17. Energy not accounted for by vaporized material.

temperature of 10,000 °K and then recondensed. If, however, 0.002 J could be accounted for in this way, this would still account for only 1% of the total energy, and would mean that ten times the amount of material that gets away from the target vaporizes and recondenses. This is unlikely. However, even if this relatively large amount is assumed and subtracted out, the shape and values for the graph of the unaccounted for energy in Figure 17, would remain about the same.

Conduction of energy into the copper target, during the time the laser is on, must also be accounted for. Ready (16) has shown, that energy can be conducted approximately 10^{-4} cm in 100 nsec in a copper target under conditions similar to these experiments. By assuming a 10,000 °K gradient across this distance, conductivity taken from handbook data at 800 °K, and an area of 2×10^{-5} cm^2, the energy used in conduction is calculated below:

$$\frac{(0.8 \frac{cal}{°K\ cm\ sec})(10^4\ °K)(2\times10^{-5}\ cm^2)(10^{-7}\ sec)(4.18\ J/cal)}{(10^{-4}\ cm)} = 7\times10^{-4}\ J$$

As can be seen, energy losses due to conduction, during the time the laser is on are negligible.

It appears then, that most of the laser beam energy must be transferred to the plume plasma or lost by reflection. Energy losses due to reflection before the power became high enough to cause a

plasma above the target would not result in continuum emission and would not be detected by the continuum measuring system. Because the laser pulses are approximately the same shape for all peak power levels investigated, it is conceivable that energy losses due to reflection before the power levels became high enough to form a plasma, could be approximately constant for the different peak powers, (11, 12, 19). As a result, energy losses due to reflection, prior to plasma formation, are assumed approximately constant as a function of laser power.

Once the plasma has begun to form, energy could be lost to the plasma directly and also after reflection from the target surface. After the plasma is formed above the target, any energy that reaches the target and is reflected will be absorbed by the plasma (11).

If these assumptions concerning energy losses are true, the shape of the function of unaccounted for energy in Figure 17 is mainly governed by energy lost to the plume plasma. As a result, the experimental graph in Figure 16 and the calculated graph in Figure 17 are both linear, giving further evidence that energy is transferred to the plume plasma in approximately a linear manner with increased laser power.

F. Non-Linearity in Ejected Material

The non-linearity in the function of ejected material shown in

Figure 14, could result from a greater efficiency of the plasma to absorb the laser beam energy as laser power increases. This efficiency could result from the increased average distance of the absorbing front from the target surface, as a function of laser power (15). Because of the small magnitude of energy used in vaporization compared to the energy transferred to the plume, this non-linearity would not appear in the energy transferred to the plume plasma.

V. SUMMARY AND CONCLUSIONS

Experimental methods were developed to monitor the power and energy of the laser beam as the target material was vaporized and collected for measurement. Also, an electronic system was built to monitor the plume plasma continuum intensity and the laser energy and power simultaneously.

Experimental measurements showed that the amount of material vaporized away from the target was not linear with laser energy and power. These data showed that the amount of material vaporized was almost independent of laser energies above 0.1 J. The amount of vaporized material was found to be small, and thus the method of analysis could be considered almost nondestructive. The amount of material was also much smaller than could be accounted for by the laser energy used.

Experimental measurements also showed a linear increase in the continuum emission of the plume plasma as a function of laser energy and power. This increase in continuum emission was shown to be related to the energy transferred to the plume plasma approximately linearly, using the product of temperature and the amount of plasma as measurement of energy content.

Energy that could not be accounted for by vaporized material, was graphed as a function of laser energy and power. It was shown,

using some reasonable assumptions, that the shape of this function is governed mainly by losses to the plume plasma. The shape of the calculated curve was found to be the same shape as the experimental one, giving evidence to the hypothesis that most of the laser beam energy is transferred to the plume plasma in approximately a linear fashion with laser power. This is energy, that might otherwise be used in vaporizing material from the target, for analytical purposes.

These experiments indicate, that little is gained analytically, in the quantity of material sampled, by increasing the power of the laser beam above 1-2 MW. Spectrographic work will be necessary to determine the effects of line emission as a function of laser beam power, due to the large amount of energy transferred to the plume rather than the target.

It is the hope of the author, that as more information becomes available on the assumptions used, that acceptance or refinements on the conclusions and interpretations of this experimental work will be made.

BIBLIOGRAPHY

1. Archbold, E., T. P. Hughes and D. W. Harper. Time resolved spectroscopy of laser-generated microplasmas. Journal of Applied Physics 15:1321-1326. 1964.

2. Barrow, Gordon M. Physical chemistry. New York, McGraw Hill, 1961. 842 p.

3. Castellan, Gilbert W. Physical chemistry. London, Addison-Wesley, 1964. 717 p.

4. Ernst, G. A fast high intensity light source for flash photoysis. Applied Optics 7:295-299. 1968.

5. Fishlook, David. A guide to the laser. New York, American Elsevier, 1967. 163 p.

6. Gregg, D. W., S. J. Thomas. Plasma temperatures generated by laser giant pulses. Journal of Applied Physics 38:1729. 1967.

7. Huddlestone, Richard H. and S. L. Leonard. Plasma diagnostic techniques. New York, Academic, 1965. 530 p.

8. Japan Electron Optics Laboratory. New application of laser microprobe. Jeol News 5:8-9. 1967.

9. Lengyel, Bela A. Lasers. New York, John Wiley, 1962. 123 p.

10. Mandelstam, S. L. et al. Optical frequency discharge in air. In: Physics of Quantum Electronics; Conference Proceedings, ed. by P. L. Kelly, B. Lax and P. E. Tannenwald. New York, McGraw Hill, 1966. p. 548-553.

11. Meyerand, R. G., Jr. and A. P. Haught. Optical-energy absorption and high-density plasma production. Physical Review Letters 13:7-9. July 6, 1964.

12. Minck, R. W. Optical frequency discharges in gases. Journal of Applied Physics 35:252-254. 1964.

13. Mocker, Hans W. and R. J. Collins. Mode competition and self-locking effects in a Q-switch ruby laser. Applied Physics Letters 7:270-273. 1965.

14. Namba, Susuma, P. Hyonkin and T. Ituh. Relative of laser induced ion energy to laser power. Japanese Journal of Applied Physics 6:273. 1967.

15. Piepmeier, Edward Harman. Spectrochemical investigation of the laser plume from an aluminum alloy target by time and spacially resolved emission and atomic absorption measurements. Ph. D. thesis. Urbana, University of Illinois, 1966. 96 numb. leaves.

16. Ready, John F. Interaction of high power laser radiation with absorbing surfaces. Address to the National Electronics Conference, Chicago, Illinois, Oct. 19-21, 1964.

17. Snetsinger, Kenneth G. and K. Keil. Microspectrochemical analysis of minerals with the laser microprobe. The American Mineralogist 52:13-26. Dec. 1967.

18. Tomlinson, R. G. Control of high brightness laser pulses through gas breakdown. Bulletin of the American Physical Society 9:729. 1964.

19. Tomlinson, R. G. Multiphoton ionization and the breakdown of noble gases. Physical Review Letters 14:489-490. 1965.

20. Vanderslice, J. T., H. W. Schamp and E. A. Mason. Thermodynamics. Englewood Cliffs, N. J., Prentice-Hall, 1966. 244 p.

21. Wright, J. K. Theory of the electrical breakdown of gases by intense pulses of light. Proceedings of the Physical Society 84:41-46. 1964.

22. Yankovskii, A. A. and V. V. Panteleev. Use of laser beams for vaporizing materials in spectral analysis. Zhurnal Prikladno: Spektroskopii 3:350-354. 1965.